Functional and structural analyses of *N*-acylsulfonamide-linked dinucleoside inhibitors of RNase A

Nethaji Thiyagarajan[1], Bryan D. Smith[2,*], Ronald T. Raines[2,3] and K. Ravi Acharya[1]

1 Department of Biology and Biochemistry, University of Bath, UK
2 Department of Biochemistry, University of Wisconsin–Madison, USA
3 Department of Chemistry, University of Wisconsin–Madison, USA

Correspondence

K. R. Acharya, Department of Biology and Biochemistry, University of Bath, Claverton Down, Bath BA2 7AY, UK
Fax: +44 1225-386779
Tel: +44 1225-386238
E-mail: bsskra@bath.ac.uk

R. T. Raines, Department of Biochemistry, University of Wisconsin–Madison, 433 Babcock Drive, Madison, WI 53706-1544, USA
Fax: +1 608 890 2583
Tel: +1 608 262 8588
E-mail: rtraines@wisc.edu

*****Present address**

Deciphera Pharmaceuticals, LLC, 643 Massachusetts Street, Suite 200, Lawrence, KS 66044-2265, USA

Molecular probes are useful for both studying and controlling the functions of enzymes and other proteins. The most useful probes have high affinity for their target, along with small size and resistance to degradation. Here, we report on new surrogates for nucleic acids that fulfill these criteria. Isosteres in which phosphoryl [R–O–P(O_2^-)–O–R′] groups are replaced with *N*-acylsulfonamidyl [R–C(O)–N$^-$–S(O_2)–R′] or sulfonimidyl [R–S(O_2)–N$^-$–S(O_2)–R′] groups increase the number of nonbridging oxygens from two (phosphoryl) to three (*N*-acylsulfonamidyl) or four (sulfonimidyl). Six such isosteres were found to be more potent inhibitors of catalysis by bovine pancreatic RNase A than are parent compounds containing phosphoryl groups. The atomic structures of two RNase A·*N*-acylsulfonamide complexes were determined at high resolution by X-ray crystallography. The *N*-acylsulfonamidyl groups were observed to form more hydrogen bonds with active site residues than did the phosphoryl groups in analogous complexes. These data encourage the further development and use of *N*-acylsulfonamides and sulfonimides as antagonists of nucleic acid-binding proteins.

Introduction

Upon catalyzing the cleavage of RNA, RNases operate at the crossroads of transcription and translation. Bovine pancreatic RNase A (EC 3.1.27.5) is the best characterized RNase. A notoriously stable enzyme, RNase A retains its catalytic activity at temperatures near 100 °C or in otherwise denaturing conditions [1], and has numerous interesting homologs [2–4]. In humans, angiogenin (RNase 5) is an inducer of

Abbreviations

PDB, Protein Data Bank; UpA, uridylyl(3′ → 5′)adenosine.

neovascularization, and plays an important role in tumor growth [5]. Eosinophil-derived neurotoxin (RNase 2) and eosinophil cationic protein (RNase 3) have antibacterial and antiviral activities. An amphibian homolog, onconase, has antitumor activity with clinical utility [6]. Even secretory RNases from the zebrafish share the RNase A scaffold [7]. Small-molecule inhibitors of these RNases could be used to investigate their broad biological functions.

The affinity of RNase A for RNA derives largely from hydrogen bonds [8], especially with the active site residues [9] and nucleobase [10]. The most potent small-molecule inhibitors of RNase A closely resemble RNA [11–17], and likewise form numerous hydrogen bonds with the enzyme. Pyrophosphoryl groups have four nonbridging oxygens, providing more opportunity for the formation of hydrogen bonds than is possible with a phosphoryl group. Accordingly, 5′-diphosphoadenosine 3′-phosphate and 5′-diphosphoadenosine 2′-phosphate exhibit strong affinity for RNase A [18], owing to extensive hydrogen-bonding interactions [19]. Pyrophosphoryl groups, however, have five rather than three backbone atoms. We reasoned that isosteres with additional nonbridging oxygen atoms but only three backbone atoms could be advantageous.

Much recent work has employed sulfur as the foundation for nucleoside linkers with multiple nonbridging oxygens. For example, achiral linkages have been made with a sulfone [R–S(O$_2$)–R′] [20], sulfonate ester [R–S(O$_2$)–O–R′] [21,22], sulfonamide [R–S(O$_2$)–NH–R′] [23], sulfamate [R–O–S(O$_2$)–NH–R′] [24], sulfamide [R–NH–S(O$_2$)–NH–R′] [25,26], and *N*-acylsulfamate [R–O–S(O$_2$)–NH–C(O)–R′] [27]. Of these functional groups, only the *N*-acylsulfamyl group has more nonbridging oxygens than does a phosphoryl group, but its length – four backbone atoms – compromises its utility as a surrogate.

We were intrigued by sulfonamides because of the relatively high anionicity of their nonbridging oxygens. Sulfonamide-linked nucleosides were employed first in antisense technology, where they were found to be highly soluble, and resistant to both enzyme-catalyzed and nonenzymatic hydrolysis [28,29]. Unlike this previous study, however, we chose to examine sulfonamides that were modified on nitrogen to install additional nonbridging oxygens.

We began our work by assessing the affinity of RNase A for two nucleic acid mimics that contain sulfonimide linkers [R–S(O$_2$)–NH–S(O$_2$)–R′], which have four nonbridging oxygens. We compared these mimics to a parent molecule that contains canonical phosphate linkers. Then, we assessed two mononucleo-

sides and two dinucleosides containing an *N*-acylsulfonamide linker [R–S(O$_2$)–NH–C(O)–R′], which has three nonbridging oxygens, in the place of a phosphoryl group. Finally, we determined the crystal structures of two *N*-acylsulfonamide-linked dinucleosides in complexes with RNase A. Together, our data lead to comprehensive conclusions regarding a new class of surrogates for the phosphoryl group.

Results and Discussion

Sulfonimides as inhibitors of RNase A

We began by determining the ability of three backbone analogs of RNA to inhibit catalysis by RNase A. These analogs have a simple polyanionic backbone with neither a ribose moiety nor a nucleobase (Fig. 1). In tetraphosphodiester **1**, three carbon atoms separate the phosphoryl groups, mimicking the backbone of RNA but without the torsional constraint imposed by a ribose ring. To reveal a contribution from additional nonbridging oxygen atoms on enzyme inhibition, we used tetrasulfonimide **2**, which has three carbon atoms between its sulfonimidyl groups, and tetrasulfonimide **3**, which has six.

Under no-salt conditions, which encourage Coulombic interactions, we could only set a lower limit of $K_i > 10$ mM for tetraphosphodiester **1** (Table 1). Previously, we reported that RNase A binds to a tetranucleotide containing four phosphoryl groups with $K_d = 0.82$ μM under low-salt conditions [30]. Thus, we
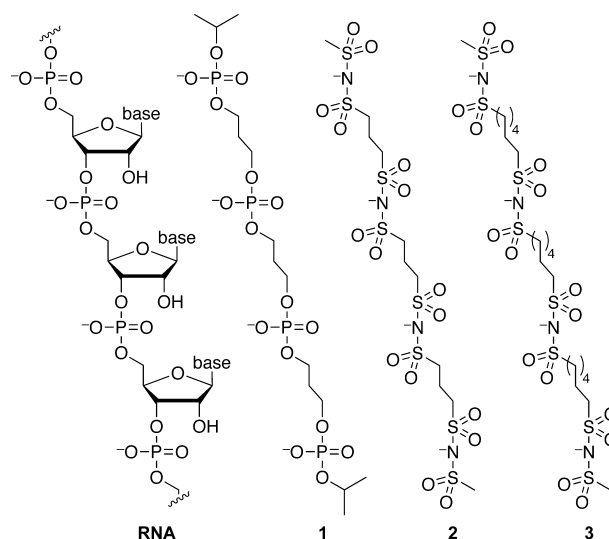

Fig. 1. Chemical structures of RNA, tetraphosphodiester **1**, and tetrasulfonimides **2** and **3**.

**Table 1.** Constants for inhibition of RNase A catalysis by compounds **1**–**7**.

Compound	K_i (mM), no salt[a]	K_i (mM), 0.10 M salt[b]
Tetraphosphodiester **1**	> 10	ND
Tetrasulfonimide **2**	0.11 ± 0.02	8.3 ± 1.7
Tetrasulfonimide **3**	0.33 ± 0.07	∼ 10
N-acylsulfonamide **4**	ND	5.3 ± 0.5
N-acylsulfonamide **5**	ND	4.8 ± 0.3
N-acylsulfonamide **6**	ND	0.46 ± 0.03
N-acylsulfonamide **7**	ND	0.37 ± 0.01

[a] Values (±standard error) in 0.05 M Bistris/HCl buffer at pH 6.0.
[b] Values (±standard error) in 0.05 M Mes/NaOH buffer at pH 6.0, containing NaCl (0.10 M).

conclude that the ribose moiety and nucleobase of a nucleic acid increase its affinity for RNase A by > 10^4-fold.

Then, we found that tetrasulfonimide **2** inhibits catalysis by RNase A with K_i = 0.11 mM under no-salt conditions (Table 1). Apparently, the additional nonbridging oxygens of tetrasulfonimide **2** provide > 10^2-fold greater affinity for RNase A. In the presence of 0.10 M NaCl, the K_i value of tetrasulfonimide **2** increased by 80-fold, indicating that binding had a Coulombic component [31,32]. This finding is consistent with RNase A (pI 9.3) [33] being cationic and each sulfonimidyl group (N–H pK_a = −1.7) [34] being anionic in aqueous solution.
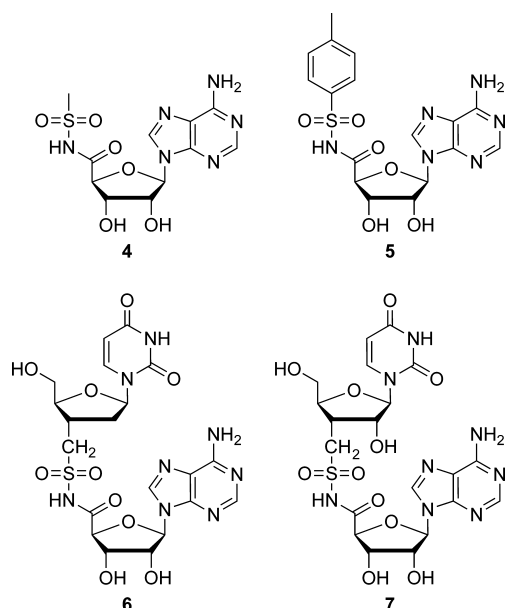
Finally, we found that tetrasulfonimide **3** inhibits catalysis with K_i = 0.33 ± 0.07 mM under no-salt conditions (Table 1). The slightly weaker affinity of tetrasulfonimide **3** than of tetrasulfonimide **2** is consistent with the spacing of their sulfonimidyl groups. RNase A has four well-defined phosphoryl group-binding subsites [35,36]. The spacing of the sulfonimidyl groups in tetrasulfonimide **2** is analogous to that of the phosphoryl groups in a nucleic acid (Fig. 1), and these sulfonimidyl groups are poised to occupy the enzymatic subsites for phosphoryl groups. In comparison, the separation between the sulfonimidyl groups in tetrasulfonimide **3** is too large.

N-Acylsulfonamide-linked dinucleosides as inhibitors of RNase A

Given the efficacy of the sulfonimidyl group as a phosphoryl group surrogate, we sought to determine the advantage of adding nonbridging oxygens to a nucleic

Fig. 2. Chemical structures of *N*-acylsulfonamide-linked nucleosides **4**–**7**.
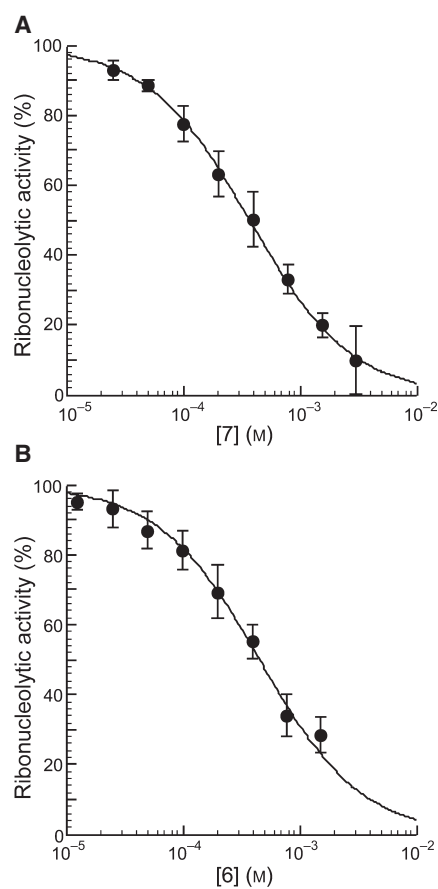
Fig. 3. Isotherms for the binding of *N*-acylsulfonamide-linked dinucleosides to RNase A. Data were fitted to Eqn (1). (A) *N*-acylsulfonamide **7**, K_i = (3.7 ± 0.1) × 10^{-4} M. (B) *N*-acylsulfonamide **6**, K_i = (4.6 ± 0.3) × 10^{-4} M.

acid. To do this, we employed an *N*-acylsulfonamidyl group, which has three nonbridging oxygen atoms and is anionic (N–H pK_a = 4–5) [34]. In compounds **4**–**7** (Fig. 2; Fig. S1), an *N*-acylsulfonamidyl group replaces the phosphoryl group in AMP or uridylyl(3′ → 5′) adenosine (UpA). We found that each of these compounds inhibited catalysis by RNase A more than did tetrasulfonimide **2** or tetrasulfonimide **3**, which are not nucleosides (Fig. 3; Table 1). The two AMP analogs inhibited RNase A with K_i values of ~ 5 mM. In contrast, AMP itself has a K_i of 33 mM [37]. The two UpA analogs inhibited RNase A with K_i values of ~ 0.4 mM (Table 1). In contrast, thymidylyl(3′ → 5′) 2′-deoxyadenosine inhibits RNase A with K_i = 1.2 mM [9]. We conclude that replacing a single phosphoryl group with an *N*-acylsulfonamidyl group confers an approximately five-fold increase in affinity for RNase A.

Of compounds **1**–**7**, RNase A binds most tightly with *N*-acylsulfonamides **6** and **7**. These inhibitors closely mimic a natural substrate for RNase A, UpA [38,39], which is cleaved by the enzyme with a rate enhancement of nearly a trillion-fold [40]. Accordingly, we decided to investigate their interactions with RNase A in detail by using X-ray crystallography.

Three-dimensional structures of RNase A·*N*-acyl-sulfonamide-linked nucleoside complexes

The three-dimensional structures of *N*-acylsulfonamides **6** and **7** in complex with RNase A were determined by X-ray crystallography (Table 2). The structures were solved to a resolution of 1.72 Å by molecular replacement in a centered monoclinic (*C*2) space group with two molecules per asymmetric unit. *N*-Acylsulfonamides **6** and **7** (Fig. 2) bound at the active site of RNase A are more fully observed in molecule A (Fig. 4). In molecule B, only adenine nucleosides are apparent (an observation similar to those made with RNase A–inhibitor complexes reported previously by us in this space group). Alternative conformations for some parts of *N*-acylsulfonamide **7**, highlighting the flexibility around the ribose moieties, are observed and are built into the structure. A similar alternative conformation was not observed for *N*-acyl-sulfonamide **6**.

Table 2. X-ray data collection and refinement statistics. $R_{symm} = \Sigma_h \Sigma_i |I(h) - I_i(h)|/\Sigma_h \Sigma_i I_i(h)$, where $I_i(h)$ and $I(h)$ are the *i*th and the mean measurements of the intensity of reflection *h*, respectively. $R_{cryst} = \Sigma_h |F_o - F_c|/\Sigma_h F_o$, where F_o and F_c are the observed and calculated structure factor amplitudes of reflection *h*, respectively. R_{free} is equal to R_{cryst} for a randomly selected 5.0% subset of reflections not used in the refinement.

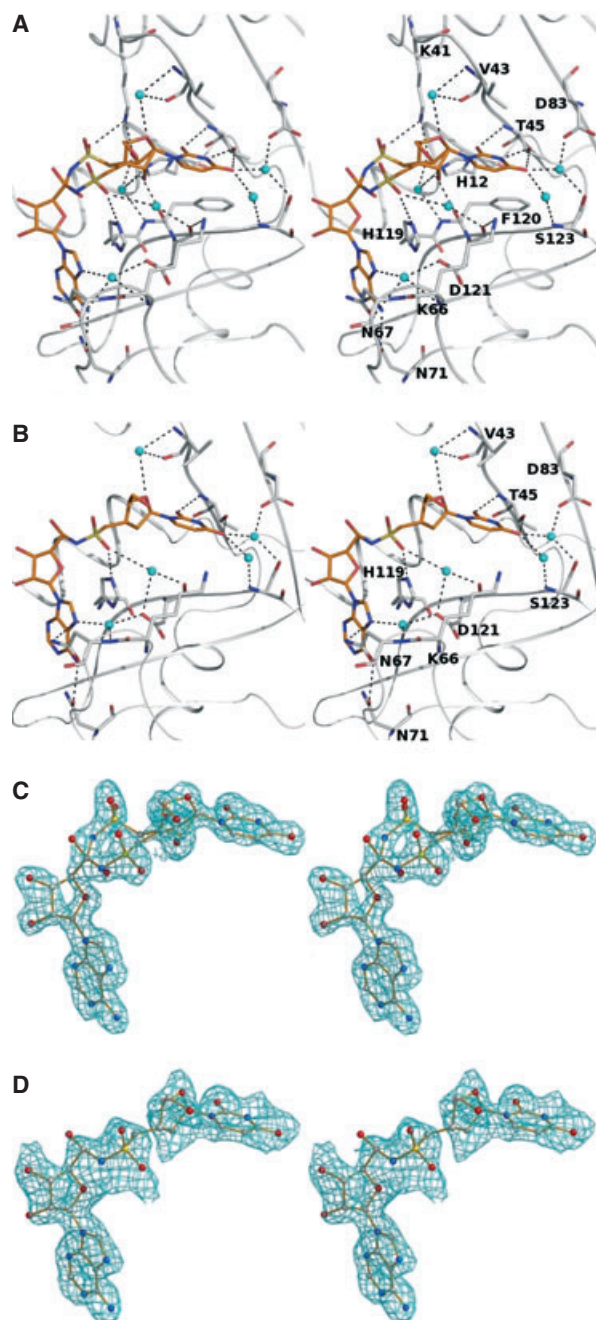|	RNase A·*N*-acylsulfonamide **7**	RNase A·*N*-acylsulfonamide **6**
Space group	*C*2	*C*2
Cell dimensions	*a* = 101.0 Å	*a* = 101.0 Å
	b = 33.1 Å	*b* = 33.2 Å
	c = 72.6 Å	*c* = 72.8 Å
	$\alpha = \gamma = 90°$	$\alpha = \gamma = 90°$
	$\beta = 90.4°$	$\beta = 90.9°$
Resolution range (Å)	50–1.72	50–1.72
R_{symm} (outer shell)	0.060 (0.171)	0.062 (0.192)
$I/\sigma I$ (outer shell)	17.5 (6.0)	17.2 (5.7)
Completeness (outer shell) (%)	98.5 (94.5)	98.0 (92.7)
Total no. of reflections	174 818	186 775
Unique no. of reflections	26 158	26 200
Redundancy (outer shell)	3.0 (2.8)	3.1 (2.9)
Wilson *B*-factor (Å^2)	17.8	18.1
R_{cryst}/R_{free}	0.212/0.246	0.214/0.244
Average *B*-factor (Å^2)		
Overall	18.1	18.3
Protein (chain A, B)	16.2, 16.5	16.4, 16.3
Ligand	21.8, 56.0	34.2, 43.2
Solvent	26.5	25.6
rmsd		
Bond length (Å)	0.007	0.007
Bond angle (°)	1.439	1.113
PDB codes	2xog	2xoi

Fig. 4. (A, B) Schematic and stereo representation of hydrogen bonds in the RNase A complex with *N*-acylsulfonamide **7** and *N*-acylsulfonamide **6**, respectively. *N*-Acylsulfonamide **7** and *N*-acyl-sulfonamide **6**, gold; active site residues, pea-green; RNase A, gray. Hydrogen bonds are represented as dashed lines, and water molecules are in cyan. (C, D) Stereo pictures of $2F_o - F_c$ contoured at 1.0σ for *N*-acylsulfonamide **7** and *N*-acylsulfonamide **6**, respectively.

N-Acylsulfonamide **6** (2′-deoxy) and *N*-acylsulfonamide **7** (2′-oxy) differ by only one atom. These two dinucleotide isosteres adopt a similar conformation

upon binding to RNase A, and occupy the same enzymic subsites as do the dinucleotides cytidylyl(3′ → 5′) adenosine [Protein Data Bank (PDB) code 1r5c] [41] and UpA (PDB code 1l1ba) [42]. The structure of *N*-acylsulfonamide **7** was refined with full occupancy, except for the alternative conformations observed for the *N*-acylsulfonamidyl group and the addition of O_2'. The value of the nucleoside torsion angle χ (Table S1) indicates that the compounds are bound in an *anti* conformation, which is the preferred orientation for bound adenine and pyrimidines [43]. The two ribose moieties exhibit a high degree of flexibility, as expected. The backbone torsion angle δ for the bound ribose units is in an unfavorable conformation, representing neither a bound nor an unbound state, although the γ torsion angle represents the bound state for ribose units with $\pm sc$. In *N*-acylsulfonamide **7**, the γ torsion angle for the ribose of adenine exhibits an unfavorable $+ac$ puckering in one of its alternative conformations.

The pseudorotation angles for the uridine of *N*-acyl-sulfonamide **7** were found in both the C_3'-*endo* (*N*) conformation and the O_4'-*endo* conformation, whereas the C_3'-*endo* conformation was preferred for *N*-acyl-sulfonamide **6**. C_3'-*endo* puckering had been observed previously for bound uridylyl(2′ → 5′)adenosine [42], 2′-CMP [44], and diadenosine 5′,5″,5‴-*P*,*P*″,*P*‴ triphosphate (Ap$_3$A) [17]. Solution NMR studies have shown that the C_3'-*endo* puckering is a predominant state for unbound furanose rings [44,45]. O_4'-*endo* puckering is an unusual conformation, and was observed in the complexes of RNase A with 2′-fluoro-2′-deoxyuridine 3′-phosphate [11] and Ap$_3$A [17] (Fig. 5).

Hydrogen bonding in RNase A·*N*-acylsulfonamide-linked nucleoside complexes

The hydrogen-bonding pattern exhibited by the nucleobases is conserved in both the 2′-oxy (**7**) and 2′-deoxy (**6**) *N*-acylsulfonamides (Table S2). In both structures, the bound inhibitors span the nucleobase-binding subsites. Surprisingly, however, the *N*-acylsulfonamidyl groups point away from the active site (Figs 4 and 5). In *N*-acylsulfonamide **7**, O_{2S} of the *N*-acylsulfonamidyl group forms hydrogen bonds with active site residues His119 and Asp121 (mediated by a water molecule). In one of its alternative states, O_{1S} of the *N*-acylsulfonamidyl group forms a hydrogen bond with Lys41. In *N*-acylsulfonamide **6**, where only a single conformation was observed for the bound *N*-acylsulfonamidyl group, O_{2S} forms two hydrogen bonds with His119 and Asp121 (mediated by a water
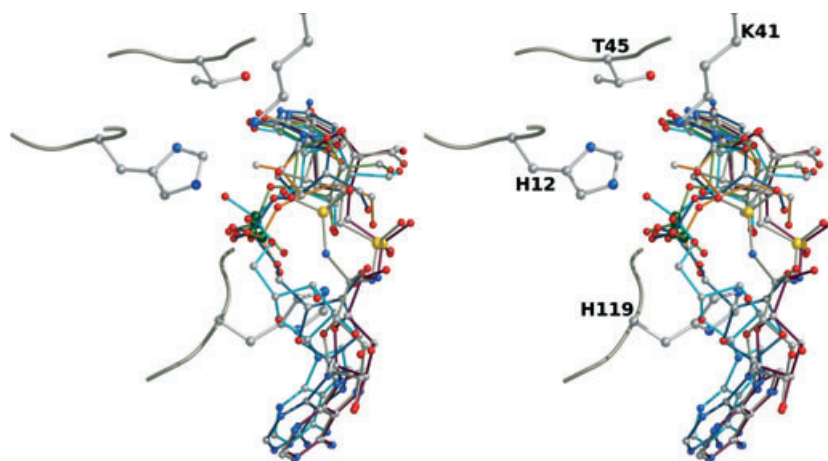
Fig. 5. Superposition (stereo representation) of *N*-acylsulfonamide **6** (gray) and *N*-acylsulfonamide **7** (maroon) (this work) on uridylyl(2′ → 5′)adenosine (cyan), cytidine 2′-phosphate (green), 2′-deoxycytidylyl (3′ → 5′)2′-deoxyadenosine (blue), and 2′-fluoro-2′-deoxyuridine 3′-phosphate (gold) (PDB codes: 11ba, 1jvu, 1r5c, and 1w4q, respectively). Sulfur atoms are in yellow; phosphorus atoms are in forest green.

molecule). Thus, replacing a phosphoryl group with an *N*-acylsulfonamidyl group leads to new hydrogen-bonding interactions.

RNase A cleaves UpA and UpG uridylyl(3′ → 5′) guanosine (UpG) with similar K_m values but significantly different k_{cat} values [46]. The similarity in the K_m values is attributable to the uracil moiety binding in the same fashion [38], which could trigger the initial binding of both substrates. In UpG, the binding of the guanine moiety is deterred by exocyclic O_6. Close inspection shows that the relevant subsite of RNase A has a negative potential and hence cannot accommodate an electronegative atom. In contrast, the exocyclic N_6-amino group of adenine forms a hydrogen bond with the side chain of Asn71, increasing the affinity of RNase A for UpA. This hydrogen bond is apparent in the complexes with *N*-acylsulfonamides **6** and **7** (Table S2; Fig. 4).

In all reported RNase A·nucleotide complexes, at least one atom of ribose (either $O_2′$ or $O_3′$) appears to interact intimately with the enzyme. The ribose unit of uridine in *N*-acylsulfonamide **7** forms four hydrogen bonds. $O_4′$ shares two hydrogen bonds with the enzyme, and $O_2′$ forms two additional hydrogen bonds in each of its conformations. Thus, in either observed conformation of *N*-acylsulfonamide **7**, there are a total of four hydrogen bonds formed by the uridine ribose. Of the two hydrogen bonds exhibited by these two atoms, one is a direct interaction with the enzyme and the other is mediated by a water molecule. In the complex with *N*-acylsulfonamide **6**, which lacks an $O_2′$, only $O_4′$ of the uridine ribose forms hydrogen bonds with the enzyme. $O_5′$ of the adenosine ribose forms a hydrogen bond with active site residue His119 in its alternative form in *N*-acylsulfonamide **7**.

Overall, *N*-acylsulfonamide **7** and *N*-acylsulfonamide **6** exhibit 12(12) and 8(11) hydrogen bonds with

RNase A (including solvent-mediated interactions in parentheses), respectively (Table S2). These numbers are comparable to those in the complexes with uridylyl(2′ → 5′)adenosine [10(5)] [42], 3′-CMP [11(2)] [46], and 2′-deoxycytidylyl(3′ → 5′)2′-deoxyadenosine [10(5)] [47]. Thus, replacing a phosphoryl group with an *N*-acylsulfonamidyl group can recapitulate, or even enhance, the characteristic structural interactions of a nucleic acid with a protein.

Conclusions

The functional and structural studies presented herein demonstrate the attributes of *N*-acylsulfonamidyl and sulfonimidyl groups as surrogates for the phosphoryl groups of nucleic acids. The structural complexes of two *N*-acylsulfonamide-linked nucleosides with RNase A closely mimic the binding by nucleic acids. The attributes and versatility of *N*-acylsulfonamidyl and sulfonimidyl groups are ripe for exploitation in the creation of nucleic acid surrogates.

Experimental procedures

A fluorogenic RNase substrate, 6-FAM–dArUdAdA–6-TAMRA (where 6-FAM is a 6-carboxyfluorescein group at the 5′-end and 6-TAMRA is a 6-carboxytetramethyl-rhodamine group at the 3′-end), was from Integrated DNA Technologies (Coralville, IA, USA). RNase A from Sigma Chemical (St. Louis, MO, USA) was used for crystallization and structure determination of RNase A·sulfonamide complexes. RNase A produced by heterologous expression [48] was used in assays to determine K_i values. All other chemicals and biochemicals were of reagent grade or better, and were used without further purification.

Compounds **1**–**3** [49,50] and **4**–**7** [51] were synthesized as described previously, and were generous gifts from T. S.

Widlanski, B. T. Burlingham, and D. C. Johnson, II (Indiana University, USA).

Determination of K_i values

Compounds **1**–**7** were assessed as inhibitors of catalysis of 6-FAM–dArUdAdA–6-TAMRA cleavage by RNase A [52,53]. Briefly, assays were performed in 2.00 mL of either 0.05 M Bistris/HCl buffer at pH 6.0 or 0.05 M Mes/NaOH buffer at pH 6.0, containing NaCl (0.10 M) that also contained 6-FAM–dArUdAdA–6-TAMRA (0.06 μM) and RNase A (1–5 pM). Mes was purified prior to use to remove inhibitory contaminants, as described previously [54]. Fluorescence (F) was measured with 493 and 515 nm as the excitation and emission wavelengths, respectively, using a QuantaMaster 1 Photon Counting Fluorometer equipped with sample stirring (Photon Technology International, South Brunswick, NJ, USA). The $\Delta F/\Delta t$ value was measured for 3 min after the addition of RNase A. An aliquot of the putative competitive inhibitor (I) dissolved in the assay buffer was added, and $\Delta F/\Delta t$ was recorded for 3 min. The concentration of I was doubled repeatedly at 3-min intervals. Excess RNase A was then added to the mixture to ensure that < 10% of the substrate had been cleaved prior to completion of the inhibition assay. Apparent changes in ribonucleolytic activity caused by dilution were corrected by comparing values with those from an assay in which aliquots of buffer were added. Values of K_i for competitive inhibition were determined by nonlinear least squares regression analysis of data fitted to Eqn (1), where $(\Delta F/\Delta t)_0$ was the activity prior to the addition of inhibitor.

$$\Delta F/\Delta t = (\Delta F/\Delta t)_0 \{K_i/(K_i + [I])\} \tag{1}$$

X-ray crystallography

Crystals of RNase A were grown by using the hanging drop vapor diffusion method [19]. Crystals of RNase A·*N*-acylsulfonamide complexes were obtained by soaking crystals in the inhibitor solution containing mother liquor [0.02 M sodium citrate buffer at pH 5.5, containing 25% (w/v) poly(ethylene glycol) 4000]. Diffraction data for the two complexes were collected at 100 K, with poly(ethylene glycol) 4000 (30% w/v) as a cryoprotectant, on station PX 9.6 at the Synchrotron Radiation Source (Daresbury, UK), using a Quantum-4 CCD detector (ADSC Systems, Poway, CA, USA). Data were processed and scaled in space group $C2$ with the HKL2000 software suite [55]. Initial phases were obtained by molecular replacement, with an unliganded RNase A structure (PDB code 1afu) as a starting model. Further refinement and model building were carried out with REFMAC [56] and COOT [57], respectively (Table 2). With each data set, a set of reflections (5%) was kept aside for the calculation of R_{free} [58]. The *N*-acylsulfonamide inhibitors were modeled with $2F_o − F_C$ and $F_o − F_C$ SIGMAA-weighted maps. The ligand dictionary files were created with the SKETCHER tool in the CCP4I interface [59]. All structural diagrams were prepared with BOBSCRIPT [60].

Acknowledgements

References

1 Klee WA & Richards FM (1957) The reaction of *O*-methylisourea with bovine pancreatic ribonuclease. *J Biol Chem* **229**, 489–504.

2 Raines RT (1998) Ribonuclease A. *Chem Rev* **98**, 1045–1066.

3 Pizzo E & D'Alessio G (2007) The success of the RNase scaffold in the advance of biosciences and in evolution. *Gene* **406**, 8–12.

4 Rosenberg HF (2008) RNase A ribonucleases and host defense: an evolving story. *J Leukoc Biol* **83**, 1079–1087.

5 Shapiro R, Riordan JF & Vallee BL (1986) Characteristic ribonucleolytic activity of human angiogenin. *Biochemistry* **25**, 3527–3532.

6 Lee JE & Raines RT (2008) Ribonucleases as novel chemotherapeutics: the ranpirnase example. *BioDrugs* **22**, 53–58.

7 Kazakou K, Holloway DE, Prior SH, Subramanian V & Acharya KR (2008) Ribonuclease a homologues of the zebrafish: polymorphism, crystal structures of two representatives and their evolutionary implications. *J Mol Biol* **380**, 206–222.

8 Fontecilla-Camps JC, de Llorens R, le Du MH & Cuchillo CM (1994) Crystal structure of ribonuclease A·d(ApTpApApG) complex. Direct evidence for extended substrate recognition. *J Biol Chem* **269**, 21526–21531.

9 Park C, Schultz LW & Raines RT (2001) Contribution of the active site histidine residues of ribonuclease A to nucleic acid binding. *Biochemistry* **40**, 4949–4956.

10 delCardayré SB & Raines RT (1995) A residue to residue hydrogen bond mediates the nucleotide specificity of ribonuclease A. *J Mol Biol* **252**, 328–336.

11 Leonidas DD, Shapiro R, Irons LI, Russo N & Acharya KR (1999) Toward rational design of ribonu-

clease inhibitors: high-resolution crystal structure of a ribonuclease A complex with a potent 3′,5′-pyrophosphate-linked dinucleotide inhibitor. *Biochemistry* **38**, 10287–10297.

12 Russo N & Shapiro R (1999) Potent inhibition of mammalian ribonucleases by 3′,5′-pyrophosphate-linked nucleotides. *J Biol Chem* **274**, 14902–14908.

13 Russo A, Acharya KR & Shapiro R (2001) Small molecule inhibitors of RNase A and related enzymes. *Methods Enzymol* **341**, 629–648.

14 Jenkins CL, Thiyagarajan N, Sweeney RY, Guy MP, Kelemen BR, Acharya KR & Raines RT (2005) Binding of non-natural 3′-nucleotides to ribonuclease A. *FEBS J* **272**, 744–755.

15 Leonidas DD, Maiti TK, Samanta A, Dasgupta S, Pathak T, Zographos SE & Oikonomakos NG. (2006) The binding of 3′-*N*-piperidine-4-carboxyl-3′-deoxy-*ara*-uridine to ribonuclease A in the crystal. *Bioorg Med Chem* **14**, 6055–6064.

16 Polydoridis S, Leonidas DD, Oikonomakos NG & Archontis G (2007) Recognition of ribonuclease A by 3′–5′-pyrophosphate-linked dinucleotide inhibitors: a molecular dynamics/continuum electrostatics analysis. *Biophys J* **92**, 1659–1672.

17 Holloway DE, Chavali GB, Leonidas DD, Baker MD & Acharya KR (2009) Influence of naturally-occurring 5′-pyrophosphate-linked substituents on the binding of adenylic inhibitors to ribonuclease A: an x-ray crystallographic study. *Biopolymers* **91**, 995–1008.

18 Russo N, Shapiro R & Vallee BL (1997) 5′-Diphospho-adenosine 3′-phosphate is a potent inhibitor of bovine pancreatic ribonuclease A. *Biochem Biophys Res Commun* **231**, 671–674.

19 Leonidas DD, Shapiro R, Irons LI, Russo N & Acharya KR (1997) Crystal structures of ribonuclease A complexes with 5′-diphosphoadenosine 3′-phosphate and 5′-diphosphoadenosine 2′-phosphate at 1.7 Å resolution. *Biochemistry* **36**, 5578–5588.

20 Huang Z, Schneider C & Benner SA (1991) Building blocks for oligonucleotide analogs with dimethylene sulfide, sulfoxide, and sulfone groups replacing phosphodiester linkages. *J Org Chem* **56**, 3869–3882.

21 Musicki B & Widlanski TS (1990) Synthesis of carbohydrate sulfonate and sulfonate esters. *J Org Chem* **55**, 4231–4233.

22 Huang J, McElroy EB & Widlanski TS (1994) Synthesis of sulfonate-linked DNA. *J Org Chem* **59**, 3520–3521.

23 McElroy EB, Bandaru R, Huang J & Widlanski TS (1994) Synthesis and physical properties of sulfonamide-containing oligonucleotides. *Bioorg Med Chem Lett* **4**, 1071–1076.

24 Huie EM, Kirshenbaum MR & Trainor GL (1992) Oligonucleotides with a nuclease-resistant sulfur-based linkage. *J Org Chem* **57**, 4569–4570.

25 Micklefield J & Fettes KJ (1997) Synthesis of sulfamide linked dinucleotide analogues. *Tetrahedron Lett* **38**, 5387–5390.

26 Micklefield J & Fettes KJ (1998) Sulfamide replacement of the phosphodiester linkage in dinucleotides: synthesis and conformational analysis. *Tetrahedron* **54**, 2129–2142.

27 Zhang J & Matteucci MD (1999) Synthesis of a *N*-acylsulfamide linked dinucleoside and its incorporation into an oligonucleotide. *Bioorg Med Chem Lett* **9**, 2213–2216.

28 Reynolds RC, Crooks PA, Maddry JA, Akhtar MS, Montgomery JA & Secrist JA III (1992) Synthesis of thymidine dimers containing internucleoside sulfonate and sulfonamide linkages. *J Org Chem* **57**, 2983–2985.

29 Maddry JA, Reynolds RC, Secrist JA, Montgomery JA & Crooks PA (1996) Polynucleotide analogs containing sulfonate and sulfonamide internucleoside linkages. *Patent* **5561225**, 1–12.

30 Fisher BM, Ha J-H & Raines RT (1998) Coulombic forces in protein–RNA interactions: binding and cleavage by ribonuclease A and variants at Lys7, Arg10, and Lys66. *Biochemistry* **37**, 12121–12132.

31 Anderson DG, Hammes GG & Walz FG Jr (1968) Binding of phosphate ligands to ribonuclease A. *Biochemistry* **7**, 1637–1645.

32 Meadows DH, Roberts GCK & Jardetzky O (1969) Nuclear magnetic resonance studies of the structure and binding sites of enzymes. 8. Inhibitor binding to ribonucleases. *J Mol Biol* **45**, 491–511.

33 Ui N (1971) Isoelectric points and conformation of proteins. I. Effect of urea on the behavior of some proteins in isoelectric focusing. *Biochim Biophys Acta* **229**, 567–581.

34 King JF (1991) Acidity. In *The Chemistry of Sulphonic Acids, Esters and Their Derivatives* (Patai S & Rappoport Z eds), pp. 249–259. John Wiley & Sons, New York.

35 Nogués MV, Moussaoui M, Boix E, Vilanova M, Ribó M & Cuchillo CM (1998) The contribution of noncatalytic phosphate-binding subsites to the mechanism of bovine pancreatic ribonuclease A. *Cell Mol Life Sci* **54**, 766–774.

36 Fisher BM, Grilley JE & Raines RT (1998) A new remote subsite in ribonuclease A. *J Biol Chem* **273**, 34134–34138.

37 Ukita T, Waku K, Irie M & Hoshino O (1961) Research on pancreatic ribonuclease. I. The inhibition of cyclic phosphodiesterase activity of bovine pancreatic ribonuclease by several substrate analogues. *J Biochem (Tokyo)* **50**, 405–415.

38 Vitagliano L, Merlino A, Zagari A & Mazzarella L (2000) Productive and nonproductive binding to ribonuclease A: X-ray structure of two complexes with uridylyl-(2′,5′)-guanosine. *Protein Sci* **9**, 1217–1225.

39 Beloglazova NG, Mironova NL, Konevets DA, Petiuk VA, Sil'nikov VN, Vlasov VV & Zenkova MA (2002) Kinetic parameters of hydrolysis of CpA and UpA sequences in an oligoribonucleotide by compounds functionally mimicking ribonuclease A. *Mol Biol (Mosk)* **36**, 1068–1073.

40 Thompson JE, Kutateladze TG, Schuster MC, Venegas FD, Messmore JM & Raines RT (1995) Limits to catalysis by ribonuclease A. *Bioorg Chem* **23**, 471–481.

41 Merlino A, Vitagliano L, Sica F, Zagari A & Mazzarella L (2004) Population shift *vs* induced fit: the case of bovine seminal ribonuclease swapping dimer. *Biopolymers* **73**, 689–695.

42 Vitagliano L, Adinolfi S, Riccio A, Sica F, Zagari A & Mazzarella L (1998) Binding of a substrate analog to a domain swapping protein: X-ray structure of the complex of bovine seminal ribonuclease with uridylyl-(2′,5′)-adenosine. *Protein Sci* **7**, 1691–1699.

43 Moodie SL & Thornton JM (1993) A study into the effects of protein binding on nucleotide conformation. *Nucleic Acids Res* **21**, 1369–1380.

44 Antonov IV, Dudkin SM, Karpeiskii MY & Yakovlev GI (1976) The conformations of phosphorylating derivatives of 2′-fluoro-2′-deoxyuridine in solution. *Sov J Bioorg Chem* **2**, 863–872.

45 Davies DB & Danyluk SS (1975) Nuclear magnetic resonance studies of 2′- and 3′-ribonucleotide structures in solution. *Biochemistry* **14**, 543–554.

46 Follmann H, Wieker H-J & Witzel H (1967) Zum Mechanismus der Ribonuclease-Reaktion. 2. Die Vorordnung im Substrat als geschwindigkeitssteigernder Faktor bei Dinucleosidphosphaten und analogen Verbindungen. *Eur J Biochem* **1**, 243–250.

47 Zegers I, Maes D, Dao-Thi MH, Poortmans F, Palmer R & Wyns L (1994) The structures of RNase A complexed with 3′-CMP and d(CpA): active site conformation and conserved water molecules. *Protein Sci* **3**, 2322–2339.

48 delCardayré SB, Ribó M, Yokel EM, Quirk DJ, Rutter WJ & Raines RT (1995) Engineering ribonuclease A: production, purification and characterization of wild-type enzyme and mutants at Gln11. *Protein Eng* **8**, 261–273.

49 Burlingham BT & Widlanski TS (2001) Synthesis and reactivity of polydisulfonimides. *J Am Chem Soc* **123**, 2937–2945.

50 Burlingham BT (2002) Design and synthesis of chemical probes for the investigation of enzyme recognition of anionic substrates. PhD Thesis, Department of Chemistry, Indiana University, USA.

51 Johnson DC II (2004) Methods for the synthesis of nucleotides and nucleoside analogs. PhD Thesis, Department of Chemistry, Indiana University, USA.

52 Kelemen BR, Klink TA, Behlke MA, Eubanks SR, Leland PA & Raines RT (1999) Hypersensitive substrate for ribonucleases. *Nucleic Acids Res* **27**, 3696–3701.

53 Park C, Kelemen BR, Klink TA, Sweeney RY, Behlke MA, Eubanks SR & Raines RT (2001) Fast, facile, hypersensitive assays for ribonucleolytic activity. *Methods Enzymol* **341**, 81–94.

54 Smith BD, Soellner MB & Raines RT (2003) Potent inhibition of ribonuclease A by oligo(vinylsulfonic acid). *J Biol Chem* **278**, 20934–20938.

55 Otwinowski Z & Minor W (1997) Processing of x-ray diffraction data collected in oscillation mode. *Methods Enzymol* **276**, 307–326.

56 Murshudov GN, Vagin AA & Dodson EJ (1997) Refinement of macromolecular structures by the maximum-likelihood method. *Acta Crystallogr* **53**, 240–255.

57 Emsley P & Cowtan K (2004) Coot: model-building tools for molecular graphics. *Acta Crystallogr* **60**, 2126–2132.

58 Brünger AT, Adams PD, Clore GM, DeLano WL, Gros P, Grosse-Kunstleve RW, Jiang JS, Kuszewski J, Nilges M, Pannu NS *et al.* (1998) Crystallography & NMR system: a new software suite for macromolecular structure determination. *Acta Crystallogr* **54**, 905–921.

59 Collaborative Computational Project, Number 4 (1994) The ccp4 suite: programs for protein crystallography. *Acta Crystallogr* **50**, 760–763.

60 Esnouf RM (1997) Bobscript: an extensively modified version of MolScript that includes greatly enhanced coloring capabilities. *J Mol Graph Model* **15**, 132–134.

Supporting information

The following supplementary material is available:

Fig. S1. Atom numbering for compounds **6** and **7**.

Table S1. Torsion angles of nucleosides in RNase A·*N*-acylsulfonamidelinked nucleoside complexes.

Table S2. Putative hydrogen bonds in RNase A·*N*-acylsulfonamide-linked nucleoside complexes.

This supplementary material can be found in the online version of this article.

Please note: As a service to our authors and readers, this journal provides supporting information supplied by the authors. Such materials are peer-reviewed and may be re-organized for online delivery, but are not copy-edited or typeset. Technical support issues arising from supporting information (other than missing files) should be addressed to the authors.